Available online at www.sciencedirect.com

ScienceDirect

Mendeleev Commun., 2013, **23**, 11–13

Mendeleev Communications

Preparation of nanocrystalline nitrogen-doped mesoporous titanium dioxide

Irina V. Kolesnik,*[a] Galina S. Chebotaeva,[a] Lada V. Yashina,[b,c] Elizaveta A. Konstantinova,[d] Andrei A. Eliseev,[a] Alexey V. Lukashin[a] and Yuri D. Tretyakov[a]

[a] *Department of Materials Science, M. V. Lomonosov Moscow State University, 119991 Moscow, Russian Federation. Fax: +7 495 939 0998; e-mail kolesnik.iv@gmail.com*
[b] *Department of Chemistry, M. V. Lomonosov Moscow State University, 119991 Moscow, Russian Federation*
[c] *State Scientific-Research and Design Institute of Rare-Metal Industry 'GIREDMET OJSC', 119017 Moscow, Russian Federation*
[d] *Department of Physics, M. V. Lomonosov Moscow State University, 119991 Moscow, Russian Federation*

DOI: 10.1016/j.mencom.2013.01.003

Nanocrystalline (4–5 nm) N-doped mesoporous TiO_2 (anatase and brookite) with N atoms in interstitial positions and a high specific surface area was prepared using hydrazine treatment and calcination in a flow of N_2.

Nanocrystalline titanium oxide is an attractive material for the photocatalytic purification of water and air to remove organic pollutants.[1] However, pure TiO_2 exhibits high photocatalytic activity only under UV-light illumination.[2] For this reason, artificial light sources such as Hg lamps are required in water and air purification systems. The doping of TiO_2 with metals[3–14] and nonmetals[15–21] changes the optical properties of TiO_2, and it may reveal photocatalytic activity under sunlight illumination.

According to published data, nitrogen is one of the most promising dopants for TiO_2, and it can raise the photocatalytic activity under sunlight by one order of magnitude.[15] Nitrogen atoms can be introduced into TiO_2 by different methods such as heating in an NH_3 flow at 1200[16] or 450–600 °C[17,18] and microwave treatment in urea solution.[19] However, these two approaches lead to an increase in the particle size; hence, the nanocrystalline TiO_2 powders do not retain their initial structure. Li *et al.*[20] have suggested another method of introducing N atoms, which includes the treatment of titanium dioxide by hydrazine with the subsequent calcination under mild conditions. Heat treatment at a low temperature allowed one to avoid the coarsening of TiO_2 particles. Here, we have applied this method to prepare N-doped nanocrystalline mesoporous titanium dioxide.

Mesoporous titanium dioxide with a disordered porous structure was prepared according to a published procedure.[21] At the first step, the hydrolysis of titanium(IV) isopropoxide (Aldrich, 97%) was performed in an aqueous solution containing Pluronic P123 block copolymer (Aldrich, 95%), HNO_3 and NH_4F (Sigma-Aldrich, 98%). The composition of the resulting mixture was $1\,Ti(OPr^i)_4 : 0.016\,P123 : 14.79\,HNO_3 : 0.01\,NH_4F : 164.35\,H_2O$. The white suspension formed after adding titanium isopropoxide was sonicated in an ultrasonic bath for 30 min and additionally stirred for 72 h at room temperature. Then, the precipitate was centrifuged and washed several times with deionized water and ethanol and dried in air. The sample was divided into two equal parts. One half was taken to remove a template by Soxhlet extraction using ethanol for 8 h. Then, both parts were calcined at 180 °C in an O_2 flow for 3 h. The samples were denoted as SE-180 (Soxhlet extraction) and OC-180 (calcined in oxygen). Both samples were soaked in hydrazine hydrate (Aldrich, 98%), dried in air and heated in an N_2 flow for 3 h at 180 and 250 °C. The samples were denoted as OCH_*T* and SEH_*T*, respectively, where *T* is calcination temperature.

The samples were characterized by X-ray powder diffraction (XRD, Rigaku D/MAX 2500 with a rotating copper anode in a 2θ range of 10–60°), silicon powder was used as an internal standard. To analyze coherent scattering domain (CSD) sizes, the profile analysis of XRD patterns was performed. Specific surface areas and pore size distributions were analyzed by N_2 sorption at 77 K (Quantachrome Nova 4200e); the isotherms were treated using BET and BJH models. The positions and concentrations of N atoms in TiO_2 were determined by XPS (Kratos AXIS Ultra DLD spectrometer, AlK_α and MgK_α irradiation) and ESR (Bruker ELEXSYS 500 spectrometer; working frequency 9.5 GHz; Xenon lamp with a UV radiation intensity of 35 mW cm^{-2} was used as an excitation light source), respectively.

The samples OC-180 and SE-180, which were used as starting materials, were studied by nitrogen sorption at 77 K and XRD (Table 1). Both samples have high specific surface areas and contain pores with an average radius of 1.7 nm and narrow size distribution. According to XRD data, the pore walls consist of nanocrystalline anatase and brookite phases with CSD sizes of 5 and 4–5 nm, respectively. The phase composition corresponded to 90% anatase and 10% brookite in the sample OC-180 and 60% anatase and 40% brookite in SE-180. Thus, Soxhlet extraction by ethanol can influence the phase composition of nanocrystalline TiO_2.We suggest that ethanol can modify the composition

Table 1 Characteristics of mesoporous N-doped TiO_2 according to low-temperature nitrogen sorption and XRD.

Sample	Specific surface area/ $m^2\,g^{-1}$	Pore volume/ $cm^3\,g^{-1}$	Average pore radius/ nm	CSD size/nm (±1 nm)		Phase composition (%) (±10%)
OC-180	280	0.36	1.7	anatase brookite	5 4	90 10
OCH-180	240	0.34	1.7	anatase brookite	5 4	70 30
OCH-250	200	0.30	1.7	anatase brookite	5 5	60 40
SE-180	270	0.34	1.7	anatase brookite	5 5	60 40
SEH-180	230	0.31	1.7	anatase brookite	5 4	50 50
SEH-250	190	0.31	1.9	anatase brookite	5 5	60 40

and structure of the amorphous phase, which may be present in as-synthesized TiO_2 so that crystallization of brookite becomes more favorable. In the other case, the crystallization of anatase from an amorphous phase is possible. In XPS and ESR spectra, the signals corresponding to N atoms in TiO_2 lattice were absent.

The changes in the structure and phase composition of hydrazine treated samples after calcination in an N_2 atmosphere were controlled by nitrogen sorption and XRD analysis (Table 1). All samples retained mesoporous structure; however, the average pore radius of SEH-250 increased from 1.7 to 1.9 nm. In turn, hydrazine treatment and calcination in an N_2 atmosphere led to a slight decrease in the pore volume and specific surface area of the samples.

According to XRD data, hydrazine treatment and calcination in N_2 results in a significant growth of the brookite content of OCH-180 and OCH-250 samples (Table 1). On the other hand, the particle size remained unchanged (4–5 nm). Therefore, we can conclude that hydrazine can influence the crystallization of an amorphous phase and lead to the preferential crystallization of brookite. In case of SE-180, the phase composition did not change significantly after hydrazine treatment and calcination. Thus, Soxhlet extraction by ethanol and hydrazine treatment with subsequent calcination cause a similar effect: the crystallization of brookite from the amorphous phase becomes more advantageous than the crystallization of anatase.

To study the state of N atoms in a TiO_2 lattice, the samples underwent XPS expertise. A peak positioned at 400 eV is present in spectra obtained for all samples treated by hydrazine [Figure 1(*a*)]. According to published data,[19] two possible positions of N atoms are characterized by different binding energies (N 1s core level): E_B = 395 eV corresponds to nitrogen in oxygen positions and E_B = 400 eV is the signal of N in interstitial positions. In terms of this interpretation, nitrogen occupies interstitial positions in all samples. A typical spectrum is presented in Figure 1(*a*). A more minor peak at 401.9 eV was observed in the XPS spectra of SEH-180 ($MgK_{\alpha 1}$ and $AlK_{\alpha 1}$ irradiation) and SEH-250 ($AlK_{\alpha 1}$ irradiation) samples [Figure 1(*b*)]. It can be attributed to interstitial nitrogen, which has a hydrogen in neighbour position (like in ammonium ion, E_B = 401.7 eV).[22] The formation of such complexes was predicted by quantum chemical calculations.[23]

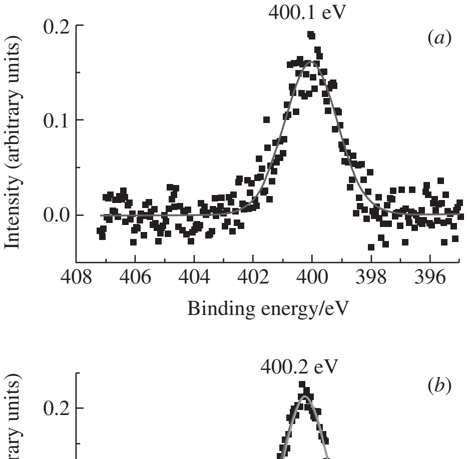

Figure 1 XPS (N1s) spectra of the sample SEH-250, (*a*) $MgK_{\alpha 1}$ and (*b*) $AlK_{\alpha 1}$ irradiation.

Table 2 XPS data for N-doped mesoporous TiO_2.

Sample	N 1s		O 1s		Ti 2p	
	E_B/eV	Concentration (at%)	E_B/eV	Concentration (at%)	E_B/eV	Concentration (at%)
OCH-180	400.0 —	< 1	530.0 531.9	63	458.7 464.4	37
OCH-250	399.9 —	<1	529.9 531.5	67	458.7 464.4	33
SEH-180	400.3/400.0[a] 401.9/402.1	2/1	531.3/531.3 530.0/529.9	67/71	458.7/458.7 464.3/464.4	31/28
SEH-250	400.2/400.1 401.9/ —	1/1	531.3/532.0 530.0/530.0 — /528.4	68/67	458.7/458.7 464.4/464.4	31/32

[a] Values which have been measured using $AlK_{\alpha 1}$ and $MgK_{\alpha 1}$ radiation are divided by slash. If only one value is present, it corresponds to $AlK_{\alpha 1}$ radiation.

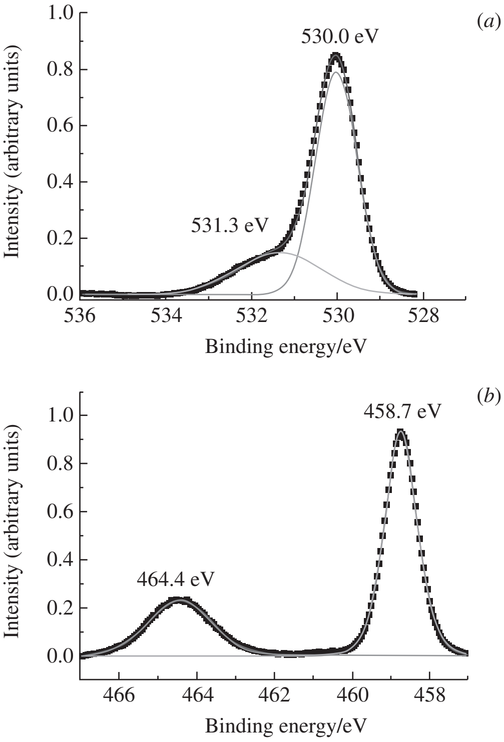

Figure 2 XPS spectra of the sample SEH-250, (*a*) O1s and (*b*) Ti2p.

A typical spectrum of O 1s level is shown in Figure 2(*a*). For all samples, the O 1s peak consists of two components with E_B = 530.0 and 531.3 eV. The first component corresponds to oxygen atoms in nanocrystalline anatase and the second one can be attributed to surface hydroxyl groups, which are always present at the surface of nanocrystalline TiO_2.[24,25]

The quantification of XPS spectra using peak intensities, relative sensitivity factors and taking into account calibrated transmission function gives rise to calculate nitrogen concentration (~1 at%) for samples after hydrazine treatment and calcination in nitrogen (Table 2).

In the Ti 2p spectra, the signals correspond to Ti^{4+} only. A peak at 458.7 eV corresponds to the Ti $2p_{3/2}$ spin-orbit component and a peak at 464.4 eV, to the Ti $2p_{1/2}$ line [Figure 2(*b*)]. Therefore, titanium atoms are not reduced to Ti^{3+}, whereas hydrazine is a strong reducing agent, or XPS is insufficiently sensitive to show a low concentration of Ti^{3+} atoms.

The EPR spectra of the sample SEH-250 measured in the dark and under illumination (Figure 3) exhibited an asymmetric signal.

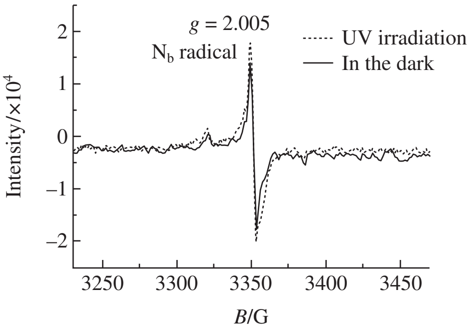

Figure 3 EPR spectra of the sample SEH-250 in the dark and under UV light irradiation.

The simulation was performed using the Symphony software with the following main parameters: g-tensor – $g_1 = 2.005$, $g_2 = 2.003$ and $g_3 = 2.002$; the EPR line width $\Delta H_1 = 3.9$ G, $\Delta H_2 = 2$ G and $\Delta H_3 = 2.8$ G and the anisotropic hyperfine tensors $A_1 = 2$ G, $A_2 = 3.2$ G and $A_3 = 32.3$ G. This signal can be attributed to such defects as N atom radicals ($N_b^\bullet$) embedded in a solid matrix.[26] When the sample is irradiated by a UV lamp, the intensity of this signal increases. The illumination effect was reversible, the EPR-signal intensity dropped to the initial value after switching off the illumination in several minutes. We assume that the N atom in a TiO_2 matrix can exist in two forms: $N_b^\bullet$ (paramagnetic) and N_b^- (charged state, diamagnetic). The latter can occur under the condition of electron transition from Ti^{3+}/oxygen vacancy centres to interstitial nitrogen atoms. Hence, Ti^{3+} centres transfer to Ti^{4+} centres in nitrogen-doped TiO_2 samples. This statement is in agreement with XPS data. The EPR-signal variations could be explained by the recharging of these defects by the following reaction:

$$N_b^- + h\nu \rightarrow N_b^\bullet + e^-. \qquad (1)$$

Thus, the presence of $N_b^\bullet$ radicals in the EPR spectra proves the introduction of N atoms in a TiO_2 lattice.

In conclusion, the treatment of nanocrystalline mesoporous titanium oxide by hydrazine with subsequent calcination in nitrogen up to 250 °C is a good low-temperature method to prepare N-doped nanocrystalline mesoporous TiO_2 with interstitial nitrogen atoms. This method does not change the pore size, pore volume and specific surface area of the samples significantly. Thus, it can be widely used to modify nanocrystalline mesoporous TiO_2 samples with N atoms without deterioration of their mesoporous structure.

We are grateful to T. V. Filippova and Dr. A. S. Vyacheslavov (M. V. Lomonosov Moscow State University) for their assistance in performing XRD and low temperature N_2 sorption experiments.

This work was supported by the Russian Ministry of Science and Education (grant no. 16.552.11.7081) and the Russian Foundation for Basic Research (grant no. 12-08-01296-a).

References

1 O. Carp, C. L. Huisman and A. Reller, *Prog. Solid State Ch.*, 2004, **32**, 33.
2 *Photocatalysis: Science and Technology (Biological and Medical Physics, Biomedical Engineering)*, eds. M. Kaneko and I. Okura, Springer-Verlag, Berlin, Heidelberg, NewYork, 2002, p. 176.
3 M. Bettinelli, A. Speghini, D. Falcomer, M. Daldosso, V. Dallacasa and L. Romano, *J. Phys. Condens. Matter*, 2006, **18**, S2149.
4 Z. Ambrus, N. Balazs, T. Alapi, G. Wittmann, P. Sipos, A. Dombi and K. Mogyorosi, *Appl. Catal. B*, 2008, **81**, 27.
5 R. A. Doong, P. Y. Chang and C. H. Huang, *J. Non-Cryst. Solids*, 2009, **355**, 2302.
6 T. J. Kemp and R. A. McIntyre, *Polym. Degrad. Stab*., 2006, **91**, 165.
7 A. Kumbhar and G. Chumanov, *J. Nanopart. Res.*, 2005, **7**, 489.
8 G. Q. Li, C. Y. Liu and Y. Liu, *Appl. Surf. Sci.*, 2006, **253**, 2481.
9 M. M. Mohamed, I. Othman and R. M. Mohamed, *J. Photochem. Photobiol. A*, 2007, **191**, 153.
10 A. M. T. Silva, C. G. Silva, G. Drazic and J. L. Faria, *Catal. Today*, 2009, **144**, 13.
11 M. Xue, L. Huang, J. Q. Wang, Y. Wang, L. Gao, J. H. Zhu and Z. G. Zou, *Nanotechnology*, 2008, **19**, 185604.
12 L. F. Zhang, D. P. He and P. Jiang, *Catal. Commun.*, 2009, **10**, 1414.
13 Y. Zhang, A. H. Yuwono, J. Wang, and J. Li, *J. Phys. Chem. C*, 2009, **113**, 21406.
14 T. K. Ghorai, S. Pramanik and P. Pramanik, *Appl. Surf. Sci.*, 2009, **255**, 9026.
15 R. Asahi, T. Morikawa, T. Ohwaki, K. Aoki and Y. Taga, *Science*, 2001, **293**, 269.
16 G. Mangamma, P. K. Ajikumar, R. Nithya, T. N. Sairam, V. K. Mittal, M. Kamruddin, S. Dash and A. K. Tyagi, *J. Phys. D: Appl. Phys.*, 2007, **40**, 4597.
17 S. Hoang, S. P. Berglund, N. T. Hahn, A. J. Bard and C. B. Mullins, *J. Am. Chem. Soc*., 2012, **134**, 3659.
18 A. Kachina, E. Puzenat, S. Ould-Chikh, C. Geantet, P. Delichere and P. Afanasiev, *Chem. Mater.*, 2012, **24**, 636.
19 F. Peng, L. F. Cai, H. Yu, H. J. Wang and J. Yang, *J. Solid State Chem.*, 2008, **181**, 130.
20 D. Z. Li, H. J. Huang, X. Chen, Z. X. Chen, W. J. Li, D. Ye and X. Z. Fu, *J. Solid State Chem.*, 2007, **180**, 2630.
21 J. C. Yu, L. Z. Zhang and J. G. Yu, *Chem. Mater.*, 2002, **14**, 4647.
22 A. V. Emeline, V. N. Kuznetsov, V. K. Rybchuk and N. Serpone, *Int. J. Photoenergy*, 2008, **2008**, 1.
23 S. P. Russo, I. E. Grey and N. C. Wilson, *J. Phys. Chem. C*, 2008, **112**, 7653.
24 G. W. Simmons and B. C. Beardt, *J. Phys. Chem.*, 1987, **91**, 1143.
25 Y. Jiang, J. Scott and R. Amal, *Appl. Catal. B*, 2012, **126**, 290.
26 E. A. Konstantinova, A. I. Kokorin, K. Lips, S. Sakthivel and H. Kisch, *Appl. Magn. Reson*., 2008, **35**, 421.

Received: 8th August 2012; Com. 12/3966